Supporting Online Material for

Pre-Fibrillar α-Synuclein Variants with Impaired β-Structure Increase Toxicity in Parkinson`s Disease Models

Damla Pinar Karpinar, Madhu Babu Gajula Balija, Sebastian Kügler, Felipe Opazo, Nasrollah Rezaei-Ghaleh, Nora Wender, Hai-Young Kim, Grit Taschenberger, Björn H. Falkenburger, Henrike Heise, Ashutosh Kumar, Dietmar Riedel, Lars Fichtner, Aaron Voigt, Gerhard H. Braus, Karin Giller, Stefan Becker, Alf Herzig, Marc Baldus, Herbert Jäckle, Stefan Eimer*, Jörg B. Schulz*, Christian Griesinger*, Markus Zweckstetter*

*** To whom correspondence should be addressed.**
E-mail: seimer@gwdg.de, jschulz4@gwdg.de, cigr@nmr.mpibpc.mpg.de, mzwecks@gwdg.de

This PDF File Includes:

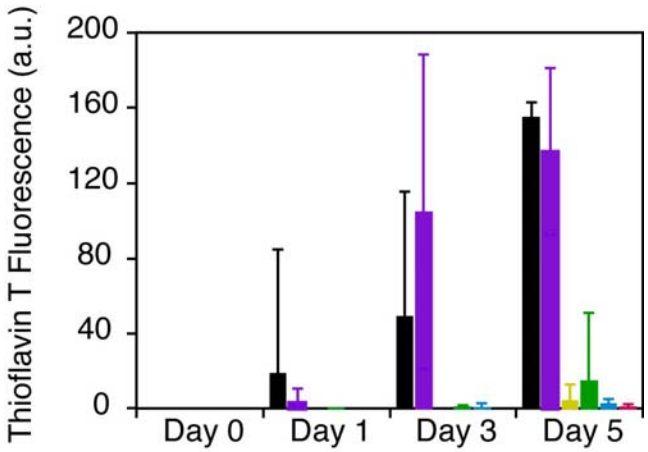

Figure S1 Thioflavin T measurements of the αS variants. *wt* (black), A30P (purple), A56P (yellow), A76P (green), A30PA56P (blue), A30PA76P (magenta).

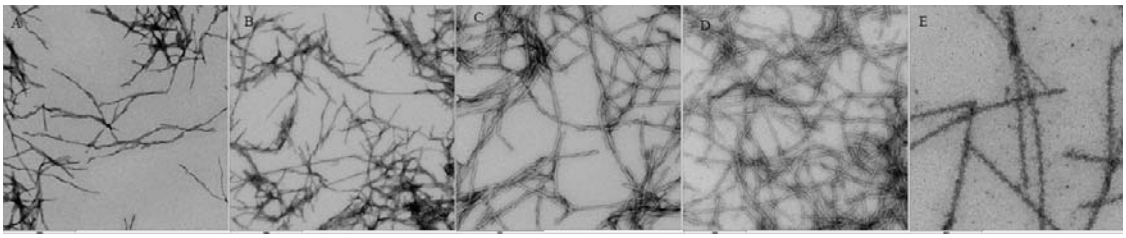

Figure S2 Electron micrographs of αS variants (A: *wt*, B: A30P, C: A53T, D: A56P, E: TP) after 5 days of incubation at 37 °C, 50 mM HEPES, 100 mM NaCl, pH 7.4 and 0.01% NaN3, stirred at 200 rpm. The protein concentration was 0.8 mM. Scale bars correspond to 1000 nm for *wt*, A30P and A53T and 500 nm for A56P and TP αS.

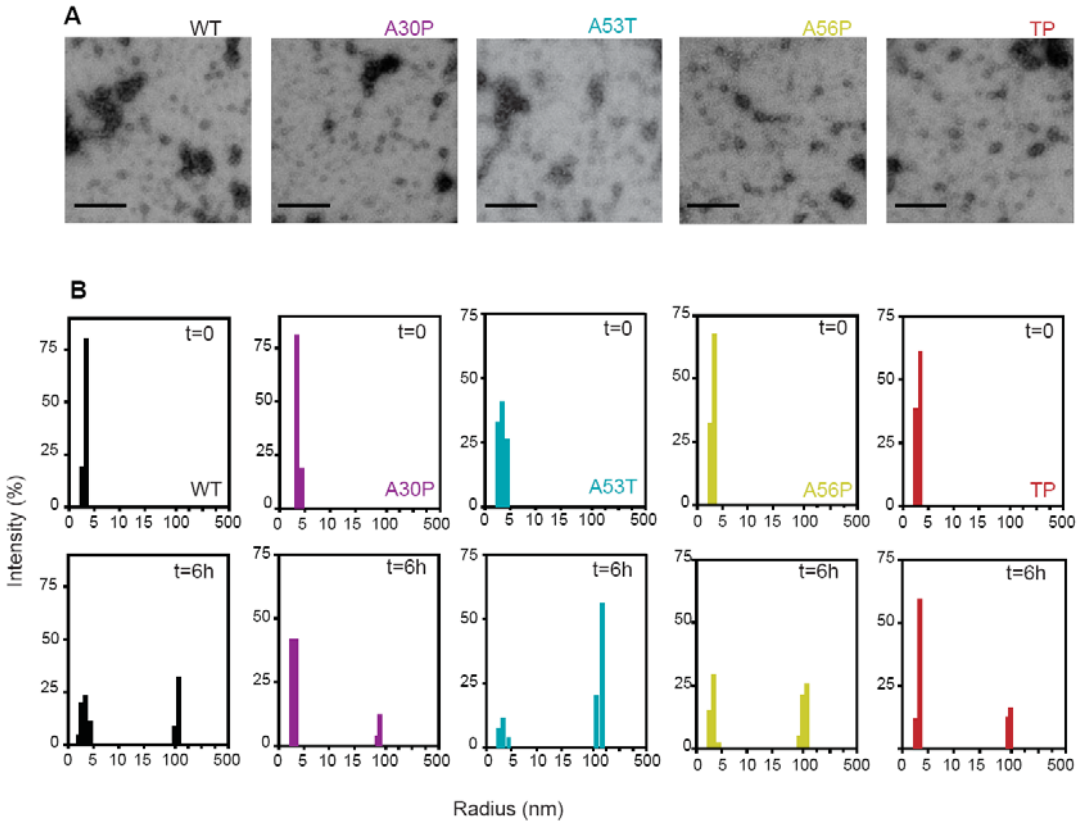

Figure S3 Morphology of soluble oligomers formed by αS variants.

(**A**) Electron micrographs of soluble oligomers formed by αS variants. The protein concentration was 100 μM and samples were aggregated for 12 h at 37 °C and 200 rpm. Scale bars correspond to 200 nm. (**B**) Dynamic light scattering of αS variants. Data presented here are a representative of 30 acquisitions of 10 s.

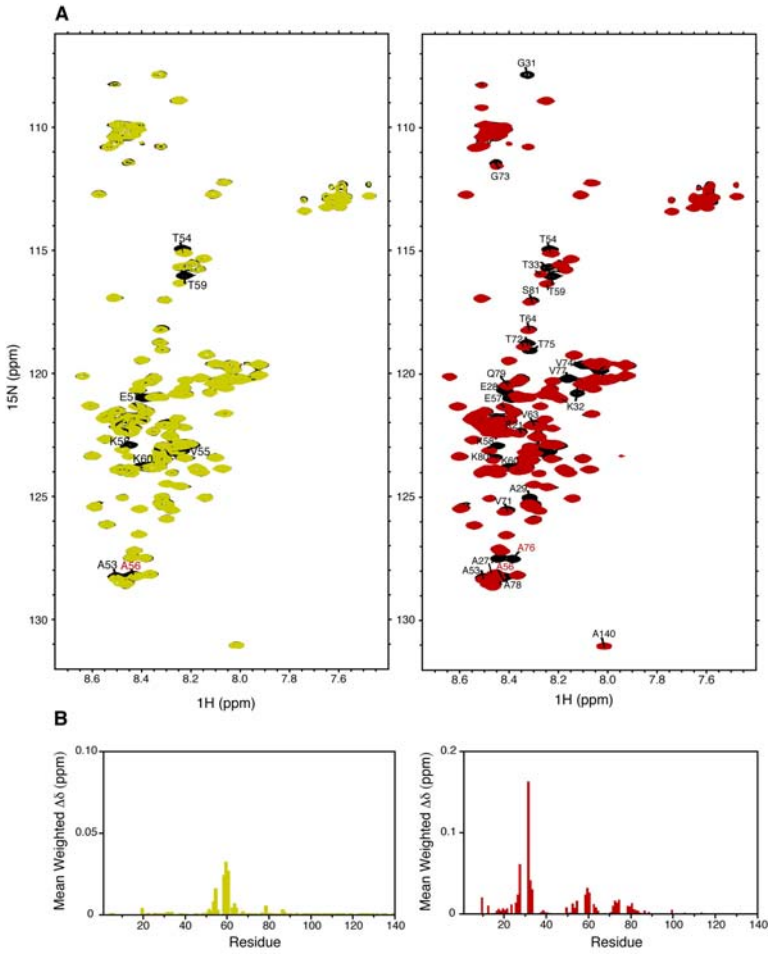

Figure S4 Monomeric forms of design variants of αS remain disordered in solution**. (A)** Superimposed contour plots of the ^{1}H-^{15}N HSQC spectra of monomeric *wt* (black), A56P (yellow) and TP (red) αS in solution at 15°C. Influenced resonances are labeled. Mutated residues are marked (red). **(B)** Mean weighted ^{1}H-^{15}N chemical shift differences between *wt* and A56P αS (yellow) and between *wt* and TP αS (red) in the free state (calculated from $[(\Delta\delta\ ^{1}H)^{2} + (\Delta\delta\ ^{15}N)^{2}/25]^{1/2}) / 2]$).

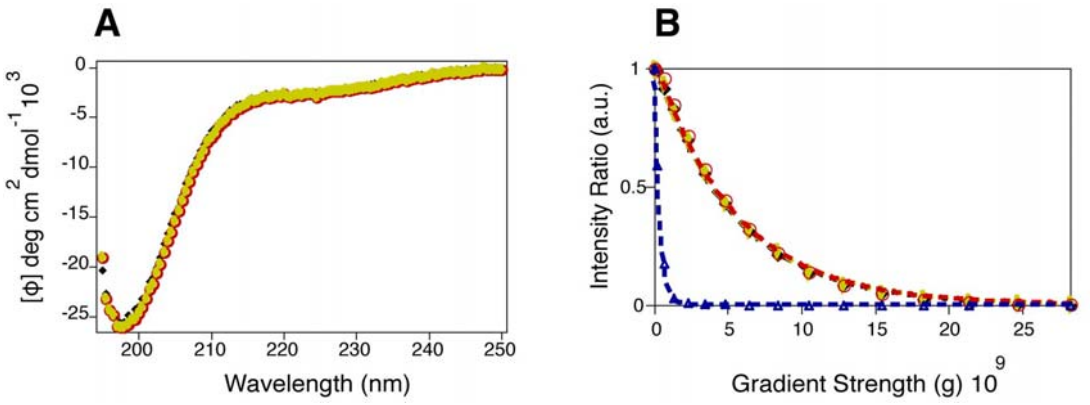

Figure S5 Secondary structure and overall shape of αS is not influenced by mutations. **(A)** Circular dichroism spectra of A56P αS (yellow), TP αS (red) and *wt* αS (black) in solution. Mutations do not substantially change the overall secondary structure of αS in the two states. **(B)** Diffusion properties of A56P αS (yellow), TP αS (red) and *wt* αS (black) as observed by NMR signal decays in pulsed field gradient measurements at 15°C. 1,4-dioxane (dark blue) was used as internal standard. The diffusion properties depend on the average hydrodynamic radius of the protein and probe the overall shape of the ensemble of conformations in solution. The fact that the diffusion properties are not substantially different in *wt* and mutant αS indicate that the overall shape averaged over the ensemble of conformations is not changed by the mutations, in agreement with SAXS measurements performed on A30P and A53T αS (Li J, Uversky VN, Fink AL. *Biochemistry*, 2001, **40**:11604-116013.)

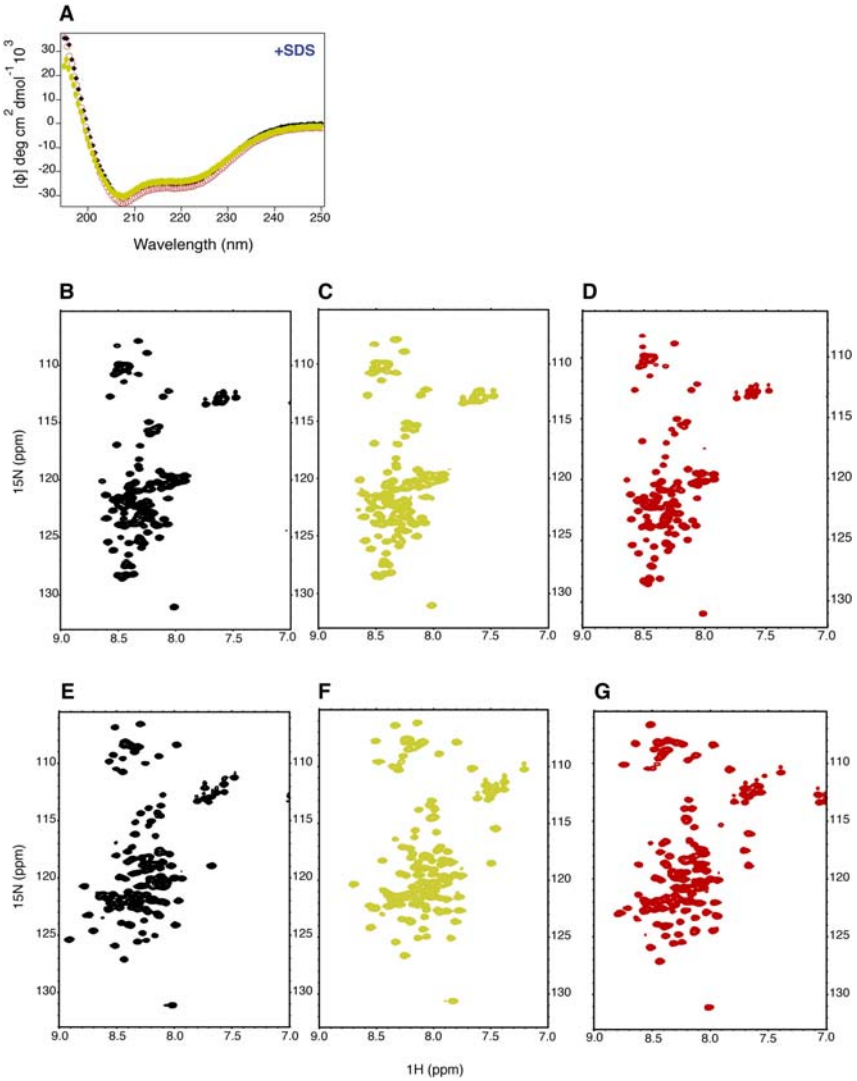

Figure S6 Design mutations do not prohibit the interaction of αS with negatively charged SDS micelles. **(A)** Circular dichroism spectra of A56P αS (yellow), TP αS (red) and *wt* αS (black) in the presence of sodium dodecyl sulfate (SDS) micelles. Transition from random coil to α-helical structure is observed for *wt* as well as the two design mutants. ^{1}H-^{15}N HSQC spectra of free *wt* (**B**), A56P (**C**) and TP (**D**) αS. ^{1}H-^{15}N HSQC spectra of *wt* (**E**), A56P (**F**) and TP (**G**) αS in the presence of SDS micelles at 40 °C and pH 7.4. An increase in resonance dispersion with respect to free spectra is observed upon addition of the micelles for all three variants.

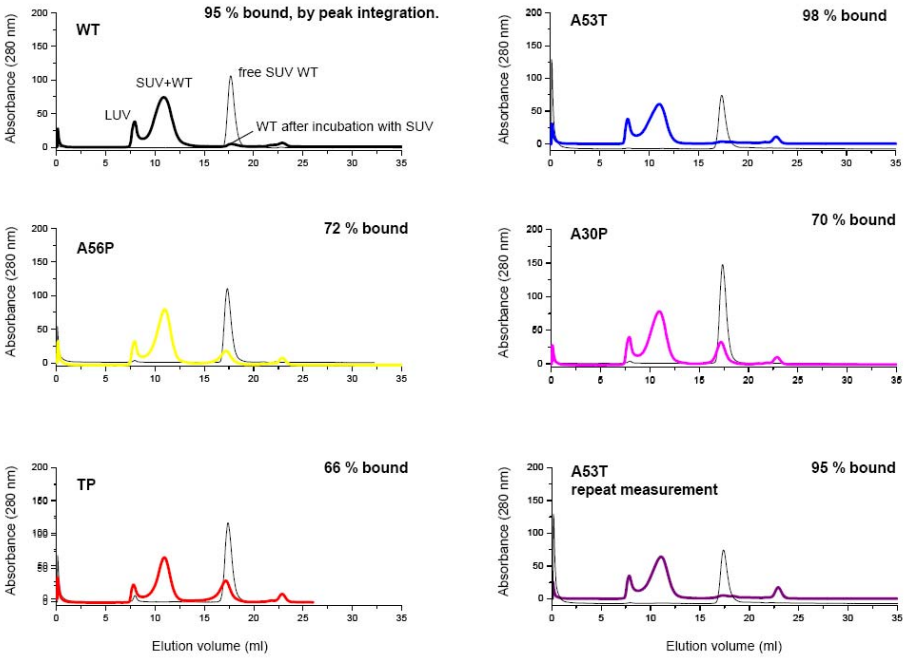

Figure S7 Binding of αS variants to phospholipid vesicles. Vesicles prepared from a 1:1 mixture of POPC and POPA were incubated for 5 hours at room temperature with αS variants at a mass ratio of 250:1, and the mixture was separated by gel filtration chromatography on a Superose 6 10/300 GL column (GE healthcare). For comparison, lipid-free αS variants (thin black line) were subjected to similar separation.

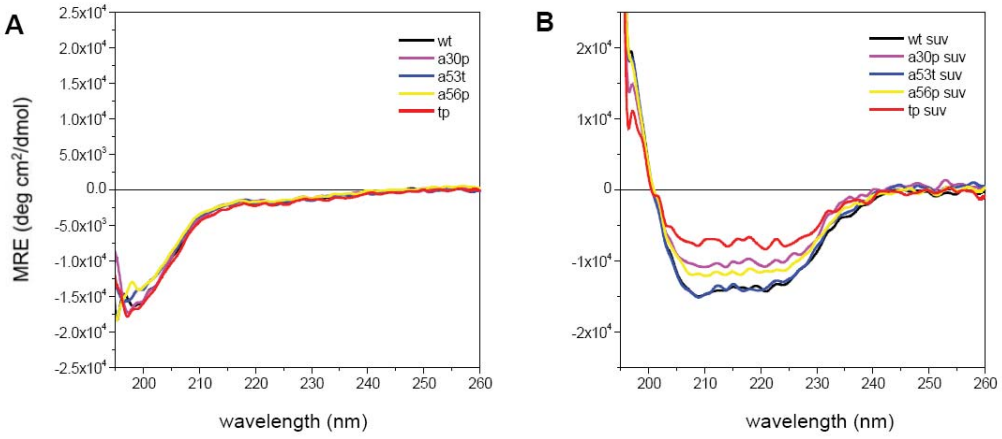

Figure S8 Circular dichorism spectra of αS variants in the free state (A) and when bound to SUVs formed by POPC:POPA (ratio 1:1) (**B**).

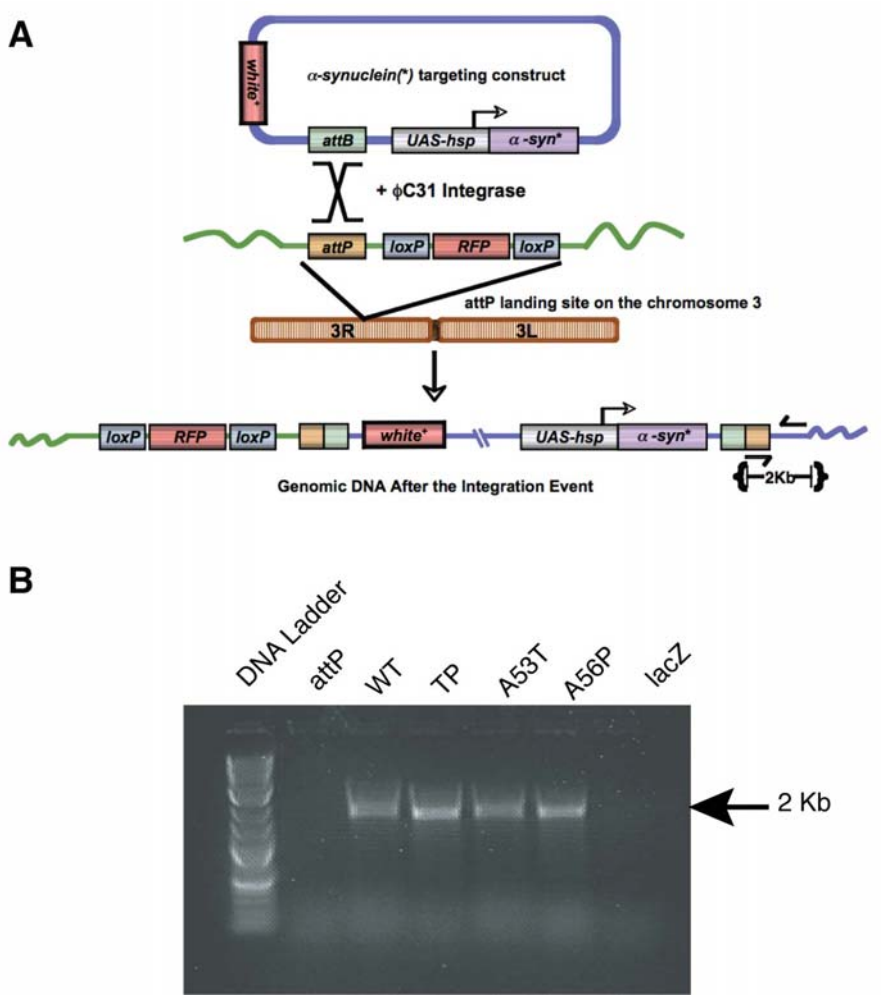

Figure S9 Targeting αS variants to an identical genomic location ensures comparable expression levels in transgenics. **(A)** Schematic representation of the *Drosophila* transgenesis based on ϕ-C31 mediated recombination. **(B)** In all transgenic animals expressing αS mutants (lanes 3,4,5,6), single fly PCR using an αS forward primer and a genomic reverse primer shows that integration has occurred at the desired attP landing site in the 3R-86Fb genomic region. As controls, flies carrying an empty-attP landing site at 3R-86Fb (lane 2) and flies carrying lacZ insertion at the same location (lane 7) were used.

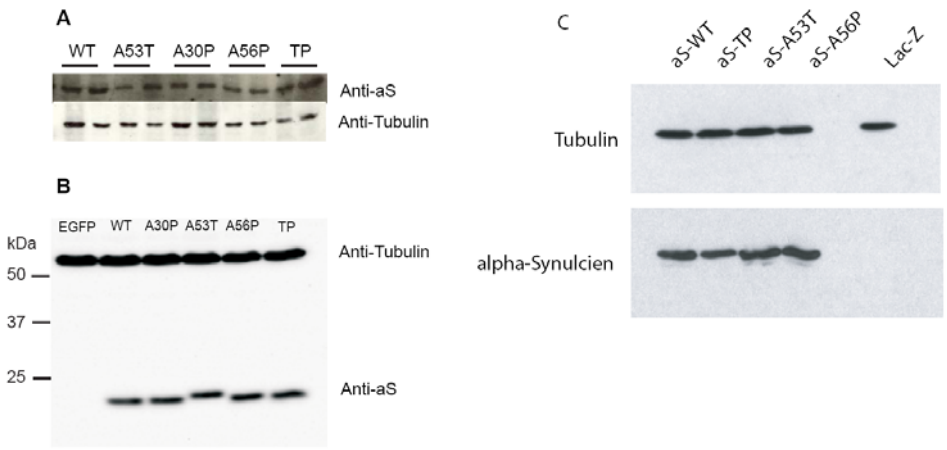

Figure S10 Expression levels of different αS variants are comparable in **(A)** *C. elegans*, **(B)** rat neuronal cultures and (**C**) fruit flies. In (B), A53T αS runs at a slightly higher molecular weight due to the presence of the seven amino acid (DTYRYI) long epitope tag AU1.

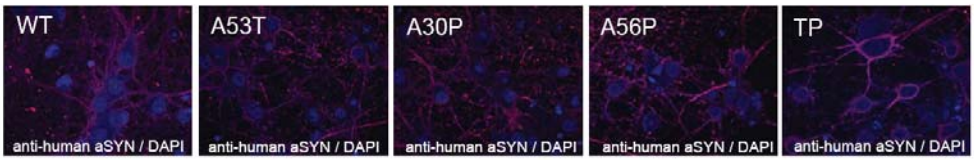

Figure S11 Immunohistochemical detection specifically of AAV-expressed human αS and variants demonstrates identical subcellular distribution of all variants: the proteins were found to be evenly distributed through cytoplasm, and within neurites demonstrated a granular staining pattern, according to a presumed localization in vesicular structures.

Table S1. α-helical content of αS variants bound to POPC:POPA SUVs.

Sample (POPC/POPA 1:1)	Secondary structure predictions by K2D* α-Helix (%)
WT	52
A30P	31
A53T	46
A56P	35
TP	27

Determined using the K2D web server (http://www.embl-heidelberg.de/~andrade/k2d.html).

Supporting Materials and Methods

Binding of aS Variants to Small Unilamellar Vesicles (SUV)

1-Palmitoyl-2-Oleoyl phosphatidyl choline (POPC) and 1-Palmitoyl-2-Oleoyl phosphatidic acid (POPA) were obtained from Avanti Polar Lipids. Vesicles were prepared from synthetic phospholipids in the following ratios: POPC/POPA (1:1). The lipids were dissolved together in a 4 ml mixture of chloroform/ methanol (1:1 vol/vol), followed by the evaporation of all solvents under a stream of N_2 gas and lyophilized overnight. The resulting lipid film was hydrated in 20 mM Tris·HCl (pH 7.4), 100 mM NaCl or in 50 mM Na-phosphate buffer (pH 7.4), 100 mM NaCl to obtain a total lipid concentration 12.5 mM. For preparation of SUV, the suspension was bath sonicated at 37 kHz (4 times for 10 min with 5 min breaks at room temperature) in a glass tube, and the SUV were isolated by ultracentrifugation at 55,000 rpm in a Beckman TLA 100.3 rotor for 2 hours at 298 K. The isolated SUV exhibited hydrodynamic diameter of 20 nm ± 5 nm from dynamic light scattering. SUVs were mixed with purified αS variants at 250:1 mass ratio of phospholipid to protein for 5 hours at room temperature, then subjected to gel filtration on a Superose 6 10/300 GL column (GE healthcare) at a flow rate of 0.5 l/min. The peak volume (detected by UV at 280 nm) at the elution position of free synuclein was integrated and compared to the corresponding peak volume obtained in the absence of SUV.

Liquid-state NMR Spectroscopy

NMR samples contained ~ 0.2 mM ^{15}N- labeled *wt* or mutant αS in 50 mM Na-phosphate buffer, 100 mM NaCl at pH 7.4 and 90% H_2O/10% D_2O. The experiments were recorded

on a Bruker Avance 600 MHz NMR spectrometer. The temperature was set to 15 °C unless otherwise stated. Data processing was performed using the software packages NMRPipe/ NMRDraw (Delaglio et al., 1995), Topspin (Bruker) and Sparky (Goddard and Kneller).

For chemical shift analysis, ^{1}H-^{15}N Heteronuclear Single Quantum Coherene (HSQC) 2D spectra were recorded (Bodenhausen and Ruben, 1980). Mean weighted ^{1}H-^{15}N chemical shift differences were calculated according to $\Delta\delta = \{[(\Delta\delta^{1}H)^{2} + ((\Delta\delta^{15}N)/5)^{2}\ ]^{1/2}\}/2$. NMR experiments on SDS micelle-bound αS were performed by addition of deuterated SDS directly to the protein sample prior to the measurement to a final concentration of 40 mM. Measurements were performed at 40 °C.

Pulse field gradient NMR experiments were performed with the PG-SLED (pulse gradient stimulated echo longitudinal encode – decode) pulse sequence (Jones et al., 1997). Sixteen one-dimensional ^{1}H spectra were collected as a function of gradient strength varying between 2% and 95% of its maximum value. Samples contained ~ 0.2 mM unlabeled *wt* or mutant αS in deuterated 50 mM Na-phosphate buffer, 100 mM NaCl at pH 7.4. As an internal hydrodynamic radius standard and viscosity probe, 0.1% 1,4-dioxane was included. After baseline correction, the decay in the intensity of the signals from the aliphatic region was fitted as a function of gradient strength (g) to the equation $f(g) = Ae^{-d(g\hat{}2)}$.

To follow the decrease in concentration of monomeric αS during aggregation, 0.5 ml samples containing 0.1 mM αS in 50 mM Na-phosphate, 100 mM NaCl, 0.1% NaN_3, pH 7.4 and 90 % H_2O / 10 % D_2O were incubated at 37 °C and stirred by 5x2 mm stirring bars inside a standard NMR tube. At appropriate time intervals, 1D ^{1}H spectra were

measured using a pulse program utilizing excitation sculpting with gradients for water suppression (Hwang and Shaka, 1995). Spectra were baseline corrected and the decay in signal intensity was plotted as a function of time. The drop in signal intensity during aggregation is due to formation of higher molecular weight aggregates not detectable by solution-state NMR. Thus, the NMR signal intensity remaining during the course of the aggregation allows estimation of the concentration of monomeric protein. Simultaneously performed EM measurements, which were performed in the early stages of the aggregation, only showed small oligomeric species and no amyloid fibrils. In addition, no increase in ThioT signal compared to the monomeric protein was detected during the lag phase. Thus, the reduction of NMR signal intensity during the lag phase of fibril formation allows estimation of the concentration of soluble oligomers. In case of the NMR aggregation assay performed for TP αS at a concentration of 0.1 mM (Figure 1C), no amyloid fibrils were detected during the complete time course of the experiment, indicating that the reduction in signal intensity is solely due to formation of soluble oligomers. Errors in the estimation of the oligomer concentration depend on the basis of the signal-to-noise ratio in the NMR spectra and are determined from the variation observed in three independently performed aggregation assays. In case of TP αS, they were ±2%.

Preparation of αS Aggregates

Recombinant human *wt* and mutant αS solutions were dialysed against 50 mM Na-phosphate buffer with 100 mM NaCl at pH 7.4 unless otherwise stated. To remove any potential seed prior to aggregation, ultracentrifugation was performed in a Beckman

ultracentrifuge equipped with TLA.100 rotor (Beckman Coulter) at 60000 rpm for 2h at 4 °C. Supernatant was filtered through 0.22 μm filter. Protein concentration was adjusted to 100 μM unless otherwise stated. 0.01% sterile filtered NaN_3 was included in the aggregation mixtures, which were then incubated in glass vials at 37 °C with constant stirring at 200 rpm on a multi-position magnetic stirring device (Variomag Telesystem 15.40, H+P Labortechnic AG, Germany). For every experiment, at least triplicates were prepared.

For seeded incubations, 200 μM solutions of TP αS were incubated for five days at 37 °C prior to seeding. Without further purification or attempt to separate monomers from oligomers, the solution, which contained monomers and oligomers of TP αS, was added to *wt* monomeric αS at an equimolar ratio. As control, we performed an aggregation assay, in which monomeric TP αS was added to monomeric *wt* αS at an equimolar ratio. Error bars in Figure 2 represent mean ± standard deviation of three to four independent experiments.

Fluorescence Measurements

Aliquots (5μl) were withdrawn from αS incubations and added to 2 ml of 5 μM ThioT in 50 mM Glycine-NaOH pH 8.2. Fluorescence measurements were carried out on a Cary Eclipse spectrofluorometer (Varian) using 3.5 ml quartz cuvettes (Hellma, Germany) with a path length of 1 cm. Aggregation yields were normalized to the final values and the averaged data points were fitted to a sigmoidal equation. (Data was represented as mean ± standard deviation, n = 3).

Dynamic Light Scattering

To monitor the build-up of oligomeric intermediates of αS, aliquots of 15 µl were withdrawn from the aggregation mixture at different time intervals and measurements were performed directly on a DynaPro Titan instrument (Wyatt Technology) at 25 °C. For the higher concentration samples (0.8 mM), 10 µl aliquots were taken at the end of incubation (11 days), then diluted 8-fold with the buffer and centrifuged at 14000 rpm for 30 minutes, and the supernatant was measured on a DLS machine. The same laser power was used for all αS variants. Data analysis was performed with the built-in software DYNAMICS from 30 successful measurements.

UV spectroscopy

After 11 days of incubation of 0.8 mM αS solutions in the aggregation condition, 10 µl aliquots were taken out and diluted 8-fold with the buffer. Thereafter, the samples were centrifuged at 14000 rpm for 30 minutes and the supernatant was investigated for apparent UV absorbance in the 210-310 nm range.

Circular Dichroism (CD) Spectroscopy

Far UV-CD measurements were performed on a Chirascan (Applied Photophysics, UK) circular dichroism spectrometer, using a protein concentration of 10 µM in 50 mM Na-phosphate, 100 mM NaCl, pH 7.4 in a quartz cuvette with 0.1 cm light-path. In case of SDS micelle samples, a concentration of 40 mM SDS was added. SUV-bound protein was prepared as described above. Each experiment was repeated at least twice. The spectral contributions of buffer and vesicles were subtracted as appropriate.

Spectrophotometric data were converted into mean residue elipticity using the internal program. Data ranging from 200 to 240 nm were used to predict α-helix content using the K2D web server (http://www.embl-heidelberg.de/~andrade/k2d.html).

Transmission Electron Microscopy

For negative staining, a solution containing protein was applied to glow-discharged carbon coated grids and stained with 1% uranyl acetate. Images were taken in a Philips CM120 electron microscope (Philips Inc.) at a defocus of 2.3 µm using a TemCam 224A slow scan CCD camera (TVIPS, Gauting, Germany).

Atomic Force Microscopy (AFM)

A TP αS solution (0.8 mM) in 50 mM HEPES, 100 mM NaCl, pH 7.4, with 0.01% NaN3 was incubated at 37 °C with stirring at 200 rpm. An aliquot of 2 µl was diluted 8-fold in the above-mentioned buffer and 4 µl of the diluted sample were deposited on freshly cleaved mica. After drying in air for 1 hr, unbound sample and buffer were washed out with 100 µl of distilled water. The samples were imaged using an Asylum MFP3D AFM machine, with a resonant frequency of about 100 kHz, a scan frequency of 1 Hz, using silicone nitride tips.

Dot Blotting

Purified recombinant proteins were spotted onto nitrocellulose membrane. Blotting was performed using the conformation-specific A11 antibody (Invitrogen´s Biosource) as described previously (Kayed et al., 2003). The amount of protein used for each spot was

10 µg. In a parallel experiment, same samples were blotted using the anti-αS antibody (BD Biosciences). The amount of the protein used was 1 µg.

Solid-State NMR Spectroscopy

For solid-state NMR measurements, 200 µM ^{13}C- and ^{15}N-labeled A56P αS was incubated for two weeks and 200 µM ^{13}C- and ^{15}N-labeled TP αS was incubated for four weeks at 37 °C and 200 rpm. Subsequently, αS aggregates were recovered by centrifugation at 60000 rpm for 2h at 4 °C (TLA.100, Beckman ultracentrifuge).

Two-dimensional NMR experiments were conducted on 14.1 T (^{1}H resonance frequency: 600 MHz) and 18.8 T (^{1}H resonance frequency: 800 MHz) NMR instruments (Bruker Biospin, Germany) equipped with 4 mm triple-resonance (^{1}H, ^{13}C, ^{15}N) MAS probes. All experiments were carried out at probe temperatures of 0 °C. MAS rates were set to values that facilitate sequential correlations at longer mixing times, i.e., 9375 Hz at 600 MHz and 12500 Hz at 800 MHz. Resonance assignments for A56P αS and a residue-specific analysis of β-strands in αS variants was based on sequential (^{13}C-^{13}C) correlation data obtained at mixing times of 150 ms (data not shown). High power proton-decoupling using the sequence SPINAL64 (Fung et al., 2000) with r.f. amplitudes of 80-90 kHz was applied during evolution and detection periods.

HEK293 cells: Control of protein expression levels .

Quantitative rtPCR. Total RNA was isolated from HEK293 cells 24h after transfection using the RNeasy Mini Kit (Quiagen, Hilden, Germany). RNA was digested by RQ1 RNase Free DNase (Promega, Mannheim, Germany) and protected against RNases by

adding 20 U of RNase Inhibitor RNasin (Promega, Mannheim, Germany). 2.5mg of total RNA was used for reverse transcriptase PCR (M-MLV; Promega, Mannheim, Germany). cDNA was diluted 1:50 and real-time reaction samples were prepared using ABsolute QPCR SYBR Green (ABgene, Hamburg, Germany), according to the manufacturer instructions. Real-time PCR was performed in a Stratagene Mx3000P Realtime device (Stratagene, La Jolla, CA). Primers for detection of a-synuclein were Fw_5′CAG GGTGTGGCAGAAGCAGC3′ and Rv_5′CTGCTGTCACACCCGTCACC3′. Eucariotic 18s ribosomal mRNA was chosen as reference gene and quantification calculated using the comparative 2-ΔΔCt method. Water and pEGFP-N1 transfected cells were used as negative controls. Three independent experiments (n=3) were performed, each with triplicates. Significance of expression differences, were tested using one-way ANOVA, which was not significant.

Western blot. Cells were plated in 6 well plates at equal density and transfected the next day. 24h after transfection, cells were harvested in phosphate buffered saline (PBS), centrifuged and resuspended in 100 µl of lysis buffer: PBS with 1% TritonX and protease inhibitor cocktail (Pierce, Rockford, IL, USA). Lysates were cleared by centrifugation (15,000 g, 20 min, 4°C) and the supernatant transferred to new tubes. 10µl of each were separated by SDS-PAGE. Primary monoclonal antibody against αS was used over night at 1:1000 and at 4°C (BD Transduction Laboratories, Cat. #610786). After incubation with the secondary antibody and visualization, the membrane was washed 3 times 20 min with stripping buffer (0.2 M Glycin, 0.5 M NaCl, pH 2.80) and incubated over night with antibody against GFP (polyclonal; Santa Cruz #SC 8334). The secondary antibodies for both primaries (GE Healthcare, #NXA931 & #NA934V) were

coupled to horseradish-peroxidase (1:10000) and visualized independently by chemiluminescence (AlphaImager, AlphaInnotech, San Leandro, CA). Quantification of αS signal was normalized against the EGFP signal of the same sample. This is a better expression control since EGFP is in the same vector but under a second CMV promotor). β-actin levels were equivalent among the different constructs, but normalizing with beta-actin would control for transfection efficiency, and not for protein expression levels. Tree independent experiments (cells plated, transfections and western blots) were performed.

C. elegans: Microscopy and behavioral analysis.

C. elegans contains eight dopaminergic neurons which are involved in food sensation (Sawin et al., 2000). These neurons have been widely used as an accepted model system to mimic Parkinson related phenotypes in *C. elegans*. As in the human system exposure of the worm to 6-hydroxydopamine (6-OHDA) or MPTP results in a specific degeneration of dopaminergic neurons and associated alterations in dopamine controlled behaviors (Braungart et al., 2004; Nass et al., 2005). Furthermore, this toxicity is dependent on the presence of the dopamine transporter DAT-1 as no degeneration is observed in *dat-1* mutant animals or if dopamine transporter inhibitors are used (Nass et al., 2005; Nass et al., 2002). Thus *C. elegans* can also be used to test and find neuroprotective compounds (Marvanova and Nichols, 2007).

Routinely, transgenic animals were imaged or assayed four days after reaching adulthood. At least three independent strains per transgene were tested. To image dopaminergic neurons, transgenic animals were anesthetized by 50mM sodium azide in M9 buffer and mounted on a 2% agarose pad. RFP positive dopaminergic neurons were

visualized using a Leica SP2 confocal microscope system. Neurite defects were scored positive if one or more dendritic processes out of four had degenerated (Nass et al., 2002). For each transgenic strain at least 75-80 animals were tested.

As a response to the presence of food wild type animals slow down their movement and reduce their area restricted searching behavior in order to feed more efficiently (Sawin et al., 2000). For behavioral analysis well-fed adult animals were transferred to the center of an assay plate with or without food as described previously (Brenner, 1974; Sawin et al., 2000). After an initial time of adjustment for 5 min the movement was assayed by counting body bends over a one min interval with three repetitions per animal. The slowing rate was calculated and defined as the percentage of locomotion on food as compared to the locomotion on plates without food. For each transgenic strain at least 35-50 animals were tested in double blind fashion. For each trail at least 35-50 transgenic animals were tested per strain in double blind fashion. Each trail was repeated tree times.

Drosophila

Longevity Assay. Flies expressing αS variants and control animals expressing *lac Z* were collected and maintained under a light-dark cycle (12 hours: 12 hours) at 25 °C with constant humidity and population density per vial. Flies were transferred to the fresh food vials and scored for survival every five days. Survival curves were calculated and plotted using Kaplan-Meier statistics, and differences between them were analysed by using the log rank method (GraphPad Prism software, San Diego, USA).

Immunohistochemistry. Whole-mount adult fly brains from the 28-30 day old animals were prepared and immuno-stained according to a previously published protocol (Wu and Luo, 2006). Rabbit anti-tyrosine hydroxylase (TH) (1:150; Chemicon International, Temecula, CA) was used to positively stain the DA neurons, and Mouse anti-nc82 (1: 200; Developmental Studies Hybridoma Bank, University of Iowa, Iowa City, IA) was used as a counter stain. From the confocal sections of fly brains of different genotypes, DM and DL clusters of DA neurons were defined and counted by using the ImageJ64 software (National Institutes of Health, Maryland, USA) (10-15 brains per genotype; two independent experiments) as described previously (Cooper et al., 2006; Sang et al., 2007).

Primary Neuronal Cultures

Primary cortical and midbrain neurons were prepared from rat embryos at E18 or E16, respectively. Neurons were plated in 96 well plates for WST assay and tyrosine hydroxylase (TH) immunocytochemistry and in 24 well plates for NeuN immunocytochemistry. Neurons were transduced by AAV vectors after three days *in vitro* (DIV 3) and were analysed at DIV 10. WST assay, measuring mitochondrial dehydrogenase activity, was performed according to the protocol of the manufacturer (Roche Diagnistics). Immunocytochemistry was performed with anti-NeuN (Chemicon) and anti-TH antibodies (Advanced Immunochemicals Inc.) detected by Cy3 coupled secondary antibody. Cell counts were performed in at least 5 randomly selected fields per well and in at least 6 wells each of at least two independent replicates of respective transduction by AxioVision software (Zeiss).

To perform statistical analysis, respective groups were tested by Levene´s test for equality of variances in order to confirm that One-Way ANOVA could be performed, for which Student-Newman-Keuls test for all pair wise comparisons was used. Data are presented as mean ± standard error of the mean (SEM).

Supporting References

Bodenhausen, G. and Ruben, D.J. (1980) Natural Abundance N-15 Nmr by Enhanced Heteronuclear Spectroscopy. *Chemical Physics Letters*, **69**, 185-189.

Braungart, E., Gerlach, M., Riederer, P., Baumeister, R. and Hoener, M.C. (2004) Caenorhabditis elegans MPP+ model of Parkinson's disease for high-throughput drug screenings. *Neurodegener Dis*, **1**, 175-183.

Brenner, S. (1974) The genetics of Caenorhabditis elegans. *Genetics*, **77**, 71-94.

Cooper, A.A., Gitler, A.D., Cashikar, A., Haynes, C.M., Hill, K.J., Bhullar, B., Liu, K., Xu, K., Strathearn, K.E., Liu, F., Cao, S., Caldwell, K.A., Caldwell, G.A., Marsischky, G., Kolodner, R.D., Labaer, J., Rochet, J.C., Bonini, N.M. and Lindquist, S. (2006) Alpha-synuclein blocks ER-Golgi traffic and Rab1 rescues neuron loss in Parkinson's models. *Science*, **313**, 324-328.

Delaglio, F., Grzesiek, S., Vuister, G.W., Zhu, G., Pfeifer, J. and Bax, A. (1995) NMRPipe: a multidimensional spectral processing system based on UNIX pipes. *J Biomol NMR*, **6**, 277-293.

Fung, B.M., Khitrin, A.K. and Ermolaev, K. (2000) An improved broadband decoupling sequence for liquid crystals and solids. *J Magn Reson*, **142**, 97-101.

Goddard, T.D. and Kneller, D.G. University of California, San Francisco.

Hwang, T.L. and Shaka, A.J. (1995) Water Suppression That Works - Excitation Sculpting Using Arbitrary Wave-Forms and Pulsed-Field Gradients. *Journal of Magnetic Resonance Series A*, **112**, 275-279.

Jones, J.A., Wilkins, D.K., Smith, L.J. and Dobson, C.M. (1997) Characterisation of protein unfolding by NMR diffusion measurements. *J Biomol NMR*, **10**, 199-203.

Kayed, R., Head, E., Thompson, J.L., McIntire, T.M., Milton, S.C., Cotman, C.W. and Glabe, C.G. (2003) Common structure of soluble amyloid oligomers implies common mechanism of pathogenesis. *Science*, **300**, 486-489.

Marvanova, M. and Nichols, C.D. (2007) Identification of neuroprotective compounds of caenorhabditis elegans dopaminergic neurons against 6-OHDA. *J Mol Neurosci*, **31**, 127-137.

Nass, R., Hahn, M.K., Jessen, T., McDonald, P.W., Carvelli, L. and Blakely, R.D. (2005) A genetic screen in Caenorhabditis elegans for dopamine neuron insensitivity to 6-hydroxydopamine identifies dopamine transporter mutants impacting transporter biosynthesis and trafficking. *J Neurochem*, **94**, 774-785.

Nass, R., Hall, D.H., Miller, D.M., 3rd and Blakely, R.D. (2002) Neurotoxin-induced degeneration of dopamine neurons in Caenorhabditis elegans. *Proc Natl Acad Sci U S A*, **99**, 3264-3269.

Sang, T.K., Chang, H.Y., Lawless, G.M., Ratnaparkhi, A., Mee, L., Ackerson, L.C., Maidment, N.T., Krantz, D.E. and Jackson, G.R. (2007) A Drosophila model of mutant human parkin-induced toxicity demonstrates selective loss of dopaminergic neurons and dependence on cellular dopamine. *J Neurosci*, **27**, 981-992.

Sawin, E.R., Ranganathan, R. and Horvitz, H.R. (2000) C. elegans locomotory rate is modulated by the environment through a dopaminergic pathway and by experience through a serotonergic pathway. *Neuron*, **26**, 619-631.

Wu, J.S. and Luo, L. (2006) A protocol for dissecting Drosophila melanogaster brains for live imaging or immunostaining. *Nat Protoc*, **1**, 2110-2115.